Recibido: 20/10/2015
Aceptado: 17/12/2015

REVISTA DE TELEDETECCIÓN
Asociación Española de Teledetección
(2015) 44, 81-89
ISSN 1133-0953
EISSN 1988-8740
http://dx.doi.org/10.4995/raet.2015.4178

CASO PRÁCTICO

Determination of agricultural land use: incidence of atmospheric corrections and the implementation in multi-sensor and multi-temporal images

Willington, E.*, Clemente, J.P., Bocco, M.

Facultad de Ciencias Agropecuarias, Universidad Nacional de Córdoba. Córdoba, Argentina.

Abstract: Soil coverage and its modifications are critical variables in human-environmental sciences. Changes in land use are causes and consequences of climate change. This situation makes that detailed and updated information is needed for many applications. Remote sensing provides data of large areas periodically, so it becomes a useful input to soil classification. The objectives of this work were to determinate algorithm and images combination that produces the best results to classify agricultural land and, simultaneously, evaluate the need of making atmospheric corrections over them, when classifying multi-temporal/multi-sensor series. The two supervised classification algorithms used were neural networks and maximum likelihood. In the study area, agriculture is the main land use, predominantly summer crops, and the area sown with soybean, corn and sorghum account for over 90% of the total. Time series of Landsat 8 and SPOT 5 images were used, and 164 plots were registered to train and validate the models as ground truth. Maximum likelihood and neural networks models produce very good results when multi-temporal/multi-sensor series are used, with global accuracy between 79.17% to 90.14% and Kappa index between 60% to 82%. The radiometric correction at surface level did not improve the results when the reflectance was corrected at the top of the atmosphere. The time series that use images taken in more advanced phenological stages of crops produce better coverage classifications than time series that use images from early stages.

Key words: Argentina, Landsat 8, maximum likelihood, neural networks, SPOT 5.

Determinación del uso del suelo agrícola: incidencia de la corrección atmosférica y la aplicación en imágenes multi-temporales y multi-sensor

Resumen: La cobertura del suelo y sus modificaciones son variables críticas para el desarrollo humano y el medio ambiente. Los cambios en el uso del suelo son causas y consecuencias del cambio climático. Estas situaciones hacen necesario contar con información detallada y actualizada. La teledetección proporciona datos de grandes áreas periódicamente, lo que hace que sea una fuente de datos importante para la clasificación de suelos. Los objetivos de este trabajo fueron determinar los algoritmos y la combinación de imágenes que producen los mejores resultados para clasificar tierras agrícolas y, simultáneamente, evaluar la necesidad de hacer correcciones atmosféricas sobre las mismas, al clasificar series multi-temporales y multi-sensor. Los dos algoritmos de clasificación supervisada utilizados fueron redes neuronales y máxima verosimilitud. En el área de estudio, la agricultura es el principal uso de la tierra, predominando cultivos de verano, y la superficie sembrada con soja, maíz y sorgo representa más del 90% del total. Se utilizaron series temporales de imágenes provenientes de Landsat 8 y SPOT 5, y 164 parcelas fueron registradas, como terreno, para entrenar y validar los modelos. Los algoritmos basados en máxima verosimilitud y en redes neuronales producen muy buenos resultados cuando se utilizan series multi-temporales e imágenes de varios sensores, con una precisión global entre 79,17% y 90,14% y un índice de

* *Autor para la correspondencia: enriquewillington@gmail.com*

Kappa entre el 60% y el 82%. La corrección radiométrica a nivel de superficie no mejoró los resultados obtenidos cuando se corrigieron reflectancias medidas al tope de la atmósfera. Las series temporales que utilizan imágenes tomadas sobre cultivos con estados fenológicos más avanzados producen mejores clasificaciones de cobertura que aquellas que utilizan imágenes de etapas tempranas.

Palabras clave: Argentina, Landsat 8, máxima verosimilitud, redes neuronales, SPOT 5.

1. Introduction

Land cover and its modifications are critical variables on important issues in human and environmental sciences; and its variations are cause and consequence of climate change. In particular it impacts on natural hydrological, climatic and geomorphologic processes. This situation makes that detailed and current information is required for many applications (Foody, 2010). Agriculture is one of the most important sectors that contribute in Argentinean economy, as a generator of foreign exchange as well as from exports and supplier of food for the domestic market (Marini *et al.,* 2007). In 2011 the agricultural complex accounted for 9% of gross domestic product in terms of exports and 42% of foreign exchange earnings (Observatorio de Economías Regionales, 2013).

Remote Sensing (RS) with multi-temporal high-resolution satellite data is an important tool used to obtain land cover information such as degradation level of forests and intensity of agricultural activities. Moreover, Geographical Information Systems (GIS) is a powerful tool in analysing spatial information. Thus, the integration of both is important to study changes in land cover patterns and dynamics in order to obtain rapid, economical, reliable and accurate results and allow a low cost crop monitoring, almost in real time, and predictions. Satellite data volumes are very large, and computer technologies to process them are in continuous evolution (Ikiel *et al.,* 2013, Bargiel and Herrmann, 2011).

The classification of land cover from satellite data is one of the most important applications in remote sensing. In fact, several new classification methods based on decision trees, bayesian networks, fuzzy systems and neural networks have been applied to satellite images with success in various contexts (Moreno-Ruiz *et al.,* 2014). In general classification methods can be grouped into parametric and non-parametric; Maximum likelihood (ML) is in the first group and has been widely used in the study area with very good statistic results, for classifying individual scenes and for time series (TS) (Nolasco *et al.,* 2014). Neural networks (NN), a very powerful and easy to implement tool belongs to the second group, can compute, process and classify information, and allow adjusting a response to non linear, complex and multi-data problems (Bocco *et al.,* 2012).

The implanted agricultural crops, with different sowing dates, predecessors and technology used, determine the heterogeneity of a studied region and define most of the classes in the classification process. It has been shown that the maximum discrimination between crops occurs at different stages in the growing season; therefore it is more difficult to determine those differences using a single date scene. In particular time series data allow detecting changes in land cover and also studying the causes (Meliadis and Miltiadis, 2011; Murthy *et al.,* 2003).

The use of time series improves the results of classifications. Multi-temporal series composed by images from two satellites were used in this work, which extends the time period of the study and adds information about the study area (Nolasco *et al.,* 2014). Cetin *et al*. (2004) made a comparative analysis to classify multi-temporal and multi-sensor series from Landsat ETM+ and Terra ASTER satellite images and their principal components, with two algorithms, ML and NN. In this case they classified eight main land-cover classes: coniferous forest, deciduous forest, urban, inland water, grassland, bare soil, road and sea.

Soybean (*Glycine max* (L.) Merr.), corn (*Zea mays* L.) and sorghum (*Sorghum bicolor* (L.) Moench) are the most important crops in Argentina, due to the sown surface and the economic returns they produce; this situation is repeated in Córdoba province, second national producer in soybean and main producer in maize and sorghum (MAGyP, 2014). In the study area this three crops represent more than 90% of the sown surface.

Table 1. Sown surface with soybean, corn and sorghum in Argentina (2013/2014).

Crop	Argentina	Córdoba
Soybean	19,781,812 ha	5,052,760 ha
Corn	6,098,885 ha	1,917,500 ha
Sorghum	997,425 ha	226,600 ha

The objectives of this work were to determinate the algorithm and the data combination that produces the better soil use classification and evaluate the need of making atmospheric corrections over the images, when classifying multi-temporal/multi-sensor series. The two supervised classification algorithms used were neural networks and maximum likelihood.

2. Materials and Methods

2.1. Study area

The study area is located in Río Segundo department, Córdoba (Argentina), it presents lightly undulated relief, a slight slope to the east (Figure 1) and silty loam soils classified as Haplustolls.

The climate is dry sub-humid, with an average annual rainfall of 800 mm and monsoon regime. The annual average temperature is 17°C. Agriculture is the main productive activity, the most frequent summer crops are soybean, corn and sorghum, and the primary method of tillage is direct seeding. Soybean varieties used are resistant to glyphosate, and maturity groups IV and V predominate, with early crops sown in November and late crops planted in December (after the wheat harvest). Corn hybrids used are resistant to *Diatraea saccaralis* Fabricius and about 60% are resistant to glyphosate. The early planting for this crop is done in the second half of September and late crops are planted from the second week of December to the first week of January. In the 2013/2014 agricultural campaign early crops of maize were not done due to drought conditions before sowing dates. Sorghum is the third main cereal crop grown in the area and is cultivated mainly by direct seeding, with early crops sown in October and late crops planted in December. To a lesser extent, wheat (*Triticum aestivum* L.) is cultivated, as a winter crop (Bocco *et al.,* 2013).

2.2. Field data and cover classes

To register the ground cover and the crops phenological stages, 14 visits to field, from October 2013 to May 2014, were performed. As ground truth, the coverage of 164 plots were taken, and from these, the different classes (Table 2) were determined.

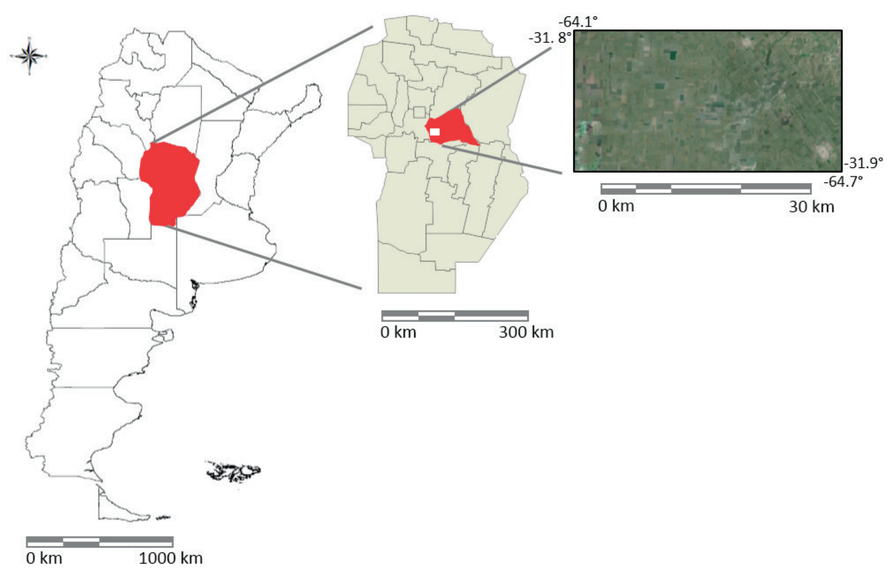

Figure 1. Study area.

Table 2. Land cover classes in Study Area (Córdoba-Argentina).

Classes	No. of ROIs	Area (ha)	Percentage (%)
Soybean	82	1952.38	57.79
Corn	36	814.49	24.11
Sorghum	15	345.13	10.22
Lucerne	10	28.74	0.85
Peanut	2	8.81	0.26
Rangelands	2	5.41	0.16
Roads	5	4.75	0.14
Water (flooded soil)	2	9.97	0.30
Bare soil and runoff channels	10	208.58	6.17

2.3. Satellite images and multi-temporal/multi-sensor series

Two images from LANDSAT 8 (L8) satellite with Standard Terrain Correction level (LT1), whose acquisition dates were 12/28/2013 (img_1) and 01/12/2014 (img_2), and two images of the satellite SPOT 5 (S5) with a correction level 2A were used. The acquisition dates of S5 images were 03/12/2014 (img_3) and 03/22/2014 (img_4), and correspond to reproductive and grain filling growth stages respectively. All images were obtained under clear sky days.

L8 images correspond to path 229, row 82, have 30 m of spatial resolution and 16 days of temporal resolution. S5 images belong to K-J 685-414 J 2A and have a spatial resolution of 10 m (except for band SWIR that has a spatial resolution of 20 m resampled to 10 m). To make the time series, a subset of all the images was creted to cover the study area, and the pixel size from L8 was adjusted to S5 (each L8 pixel is divided into nine parts with the same attribute value). Before making the time series, twenty points that belong to the registered plots were used as ground control points. This procedure ensured that there were no deviations between the images. As a result the spatial resolution for the series is 10 m.

Radiometric correction was made in two steps. In the first step, from digital counts (DC) to reflectance at the top of atmosphere (TOA_Ref), in a second step, from TOA_Ref to land surface reflectance (Sur_Ref), using the method of dark object subtraction (Chavez Jr., 1988). The time series were created by the layer stacking technique and were named according to their level of correction; the first set named TS_x_TOA and the second TS_x_Sur (where x indicates the numbers of the images included in the series, i.e. TS_432_TOA is formed with img_4, img_3 and img_2 and data were corrected at the top of atmosphere). Each image used included all the available data; bands 1, 2, 3, 4, 5, 6 and 7 of L8 or bands XS1, XS2, XS3 and SWIR of S5.

Figure 2 shows an illustrative diagram of the four images and the resulting time series (four corrected at top of atmosphere and four at land surface). The series, eight in total, included data from two, three or four images and each one was classified

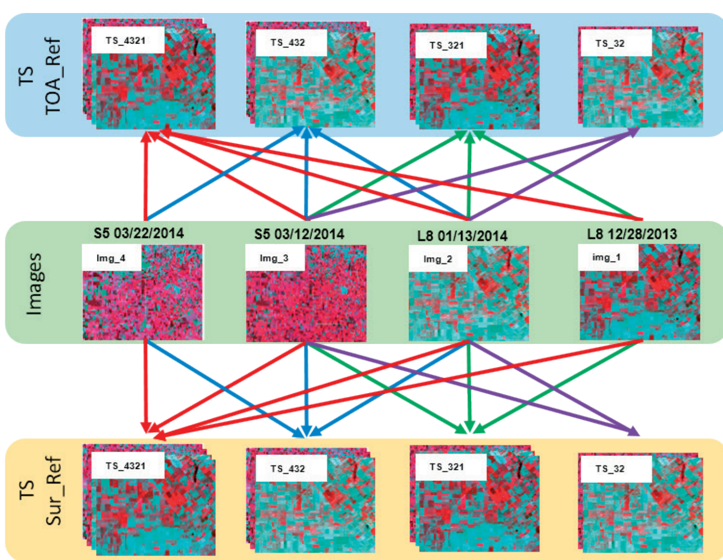

Figure 2. Images and time series (with radiometric correction).

with two methodologies, resulting 16 classified scenes.

Image processing (subset, radiometric corrections, layer stacking), classifications and the post classification statistical analysis were performed using the software ENVI 4.6.1 (Exelis Visual Information Solutions, Boulder, Colorado).

2.4. Supervised classification

Regions of interest (ROI) were formed digitizing 164 polygons on the study area, 82 were used to classify and 82 to validate both methodologies, maximum likelihood and neural network. All available bands for both satellites were used in the classifications (Table 3).

Maximum likelihood: It is a parametric method widely used for its simplicity and speed of calculation, based on the use of the variance-covariance vector to estimate the probability of a pixel to belong to a class. Classifications were done with a single probability threshold value and a scale factor data equal to 1.00.

Neural Networks: are mathematical models widely used to classify images. They simulate the behaviour of neurons in the human brain by replicating, on a small scale, the brain's patterns in order to produce results from the events perceived. NN are a structure of neurons joined by nodes that transmit information from one neuron to another, which gives a result by means of mathematical functions (Hilera-González and Martínez-Hernando, 2000).

This classification method is characterized by not making assumptions about the data statistical distribution. All NN models were constructed with three neurons layers, the input layer was formed by the bands present in the time series, the hidden layer had the same number of neurons and the output layer indicates the land use. A detailed description of the NN methodology is done in Bocco *et al*. (2014). The training included the following parameters: logistic activation function, training threshold 0.9, training rate 0.2 and training momentum 0.9. Training criteria for convergence was met with a mean squared error equal to 0.10 or a maximum of 1000 iterations.

Table 3. Bands images and their properties used in classifications.

Satellite	Spectral bands	Wavelength	Spatial resolution
SPOT 5	XS1	0.495 to 0.605 µm	10 m
	XS2	0.617 to 0.687 µm	10 m
	XS3	0.780 to 0.893 µm	10 m
	SWIR	1.545 to 1.750 µm	20 m*
LANDSAT 8	Band 1	0.433 to 0.453 µm	30 m
	Band 2	0.450 to 0.515 µm	30 m
	Band 3	0.525 to 0.600 µm	30 m
	Band 4	0.630 to 0.680 µm	30 m
	Band 5	0.845 to 0.885 µm	30 m
	Band 6	1.560 to 1.660 µm	30 m
	Band 7	2.100 to 2.300 µm	30 m

*Resampled to 10 m.

2.5. Statistical analysis

The classifications accuracy was evaluated through the analysis of the confusion matrices, being widely used to validate classifications. (Willington *et al.,* 2013). For each classification model, global accuracy and kappa index values were obtained from the observed and estimated data. The formulas are:

Global accuracy:
$$Ga = \frac{\sum_{i=1}^{m} x_{ii}}{N}$$

Kappa index:
$$\kappa = \frac{N \sum_{i=1}^{m} x_{ii} - \sum_{i=1}^{m} x_{i\Sigma}\ x_{\Sigma i}}{N^2 - \sum_{i=1}^{m} x_{i\Sigma}\ x_{\Sigma i}}$$

Where m=total number of classes, N=total number of pixels in the m reference class, xii=elements in the main diagonal in the confusion matrix, $x\Sigma\ i$=sum of the pixels in the i reference class, and $xi\Sigma$=sum of the classified pixels as i class.

Ga indicates the number of pixels of all classes of coverage that were correctly classified in relation to the total number of reference pixels, expressed in percentage.

Kappa index computes the agreement between the classified image and the ground truth, only because of the classification accuracy, not considering the agreement that would be expected by random. Monserud and Leemans (1992) proposed a scale to interpret the *κ* values; less than 40% are poor, 40 to 55% are sufficient, 55 to 70% are good, 70 to 85% are very good and higher than 85% are excellent.

Besides from the confusion matrices producer accuracy (PA) and user accuracy (UA) values are calculated as explained by Congalton (1991).

3. Results and Discussion

The results show that both methodologies, ML and NN, allow good classifications, particularly when the three images correspondent to more advanced crop phenological stages were used. These correspond to more advanced phenological crop stages than img_1; in this last one, the reflectance is from an interface soil/vegetation,, which does not contribute to improve the classification performances. Table 4 shows the statistics obtained from the classifications confusion matrix.

Table 4. Statistics obtained by the models, sorted by *Ga* and *κ* values.

Temporal serie	Model	*Ga* (%)	*κ* (%)
TS_432_Sur	ML_6	90.14	82
TS_432_TOA	ML_2	90.14	82
TS_32_TOA	NN_4	88.55	79
TS_4321_Sur	ML_5	88.38	78
TS_4321_TOA	ML_1	88.38	78
TS_321_Sur	ML_7	88.25	77
TS_321_TOA	ML_3	88.25	77
TS_432_Sur	NN_6	87.64	77
TS_32_TOA	ML_4	86.99	76
TS_32_Sur	ML_8	86.99	76
TS_32_Sur	NN_8	82.58	69
TS_4321_TOA	NN_1	81.89	65
TS_321_TOA	NN_3	80.99	62
TS_432_TOA	NN_2	80.75	63
TS_4321_Sur	NN_5	79.86	61
TS_321_Sur	NN_7	79.17	60

When comparing the performance of the two classification algorithms, the highest values of *Ga* were for ML_6 and ML_2 (both use data from the same images), NN_4 (which uses data from img_2 and img_3) is in the third place of exactitude; the remaining ML and NN models have lower precision values. In general ML models present κ values classified as very good, while NN models are classified as very good or good. Cetin *et al.* (2004) classified multi temporal/multi sensor images using NN and ML, and obtained *κ* values that ranged between 0.89 to 0.96 and from 0.84 to 0.92 respectively. Murthy *et al.* (2003) compared NN and ML to classify wheat from other crops in multi temporal images, using digital counts, and obtained better results for NN than ML when land cover was classified into four classes: wheat, oilseeds, other crops and fallow lands.

Analyzing the best combination of images to use, it is seen that the two classifications that give the best results (ML_6 and ML_2) use data from three images, the two images of March and one of January (Figure 3). ML_5 y ML_1 models add the img_1, however, the use of this fourth image does not produce better results.

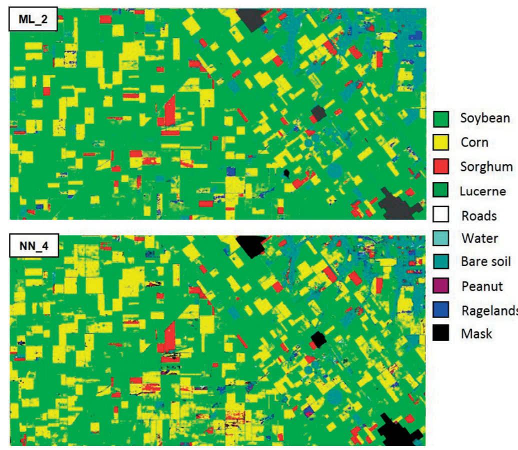

Figure 3. Classifications images with ML_2 and NN_4 models.

Guerschman *et al.* (2003) used multi temporal Landsat TM data to classify land cover in Buenos Aires province (Argentina) and obtained their greatest statistical values (*Ga*=62.6% and *κ*=54.7%) when used all available bands (3, 4 and 5) of four images. Marini *et al.* (2007) determined land use in Guaminí (Buenos Aires, Argentina) from Landsat time series. They used NDVI and decision trees and achieved an overall accuracy of 87.96% and *κ* index of 0.85; equivalent values to the obtained in the present paper.

Among the NN models, NN_4 presents the highest *Ga* value. It uses data from two images corrected at top of atmosphere and its *κ* value is very good. Besides, it is noted that the classifier achieves very good results with data from only two images.

If the analysis is focused on the correction level of the temporal series, the results of using reflectance at surface level or at the top of atmosphere are equal for ML models (Table 4). On the other hand, NN models have another behavior and there are differences when images were corrected at top of atmosphere or at surface level. In general NN models corrected at the top of atmosphere have better statistics than NN models corrected at surface level, except for NN_6 in comparison to NN_2. These results are consistent with Murthy *et al*. (2003), who compared the digital numbers of pseudo invariant objects (deep water bodies, highways, etc) from the images that form the time series and found that the effect of atmosphere on the multi-temporal data is not significant.

In the study area the main three crops (soybean, corn and sorghum) represent more than 90% of the sown surface (Table 2). When analyzing the PA and the UA values it is observed that more than 90% of soybean pixels are classified correctly, independently of the classification algorithm or the temporal series used.

On the other hand, Table 5 shows that the best two models (ML_2 y NN_4) ensure with probability over 93% that a pixel classified in a class belongs effectively to that class for the three main crops. Among all models, that uses only two images (NN_4) presents the best producer accuracy for corn class. As the presence of sorghum is significantly lower that the crops mentioned (10%), ML_2 and NN_4 present lower probabilities that a pixel of sorghum is classified as such; however, the user accuracy for this crop presents equivalent values than soybean class.

Table 5. Producer and user accuracy for the best models and the main crops.

Classified Coverage	ML_2		NN_4	
	PA	UA	PA	UA
Soybean	92.90	93.50	91.77	93.30
Corn	89.94	86.02	91.98	80.43
Sorghum	59.99	94.05	51.26	93.12

It should be noted that while the ML models produced good global performance, when each classified category is analyzed errors are observed in some of them. For example, ML_4 and ML_8 models present a large increase in the percentage of pixels classified as roads, however their global accuracy and kappa values are good (86.99 and 76% respectively), reaching both models more than 14% for this class (Figure 4). The neural networks, by contrast, never showed results with a significant percentage of pixels misclassified as roads; between these, NN_7 presents the highest value (2%) of pixels classified as roads.

Figure 4. Classification image with ML_4 model (high roads cover).

4. Conclusions

Maximum likelihood and neural networks models produce very good results when multi-temporal/multi-sensor series are used to classify land use. The time series that use images taken in more advanced phenological stages of crops produce better coverage classifications than time series that use images from early stages.

The series formed by two images produce very good results, for maximum likelihood and neural networks. This can be useful in years with problems in image acquisition, i.e. when there is high proportion of cloudiness.

The radiometric correction at surface level did not improve the results obtained when the reflectance was corrected at the top of the atmosphere.

It is expectable that the atmospheric correction at ground level produced better or at least equal results in the classifications. This did not occur for NN models. Further research should be done in order to explain the causes of these results, mainly regard to the dark object subtraction method used in the study area.

Acknowledgements

The authors express their gratitude to the FCA-UNC and SECyT-UNC for financial support that allowed the realization of this work. And especially to Ing. Agr. Miguel Nolasco, who assisted in data recording stage of this investigation.

References

Bargiel, D., Herrmann, S. 2011. Multi-temporal land-cover classification of agricultural areas in two European regions with high resolution spotlight TerraSAR-X data. *Remote Sensing,* 3(5), 859-877. http://dx.doi.org/10.3390/rs3050859

Bocco, M., Ovando, G., Sayago, S., Willington, E., Heredia, S. 2012. Estimating soybean ground cover from satellite images using neural-networks models. *International Journal of Remote Sensing,* 33(6), 1717-1728. http://dx.doi.org/10.1080/01431161.2011.600347

Bocco, M., Ovando, G., Sayago, S., Willington, E. 2013. Simple models to estimate soybean and corn percent ground cover with vegetation indices from modis. *Revista de Teledetección* 39, 83-91. Available at http://www.aet.org.es/revistas/revista39/Numero39_07.pdf (accessed December 2015).

Bocco, M., Sayago, S., Willington, E. 2014. Neural network and crop residue index multiband models for estimating crop residue cover from Landsat TM and ETM+ images. *International Journal of Remote Sensing*. 35(10), 3651-3663. http://dx.doi.org/10.1080/01431161.2014.915436

Cetin, M., Kavzoglu, T., Musaoglu, N. 2004. Classification of multi-spectral, multi-temporal and multi-sensor images using principal components analysis and artificial neural networks: Beykoz case. *International Society for Photogrammetry and Remote Sensing*. Available at http://www.isprs.org/proceedings/XXXV/congress/comm4/papers/480.pdf (accessed July 2015).

Chavez, P.S. Jr. 1989. Radiometric calibration of Landsat Thematic Mapper multispectral images. *Photogrammetric Engineering and Remote Sensing* 55, 1285-1294.

Congalton, R.G. 1991. A review of assessing the accuracy of classifications of remotely sensed data. *Remote sensing of Environment,* 37(1), 35-46. http://dx.doi.org/10.1016/0034-4257(91)90048-B

Foody, G.M. 2010. Assessing the accuracy of land cover change with imperfect ground reference data. *Remote Sensing of Environment,* 114(10), 2271-2285. http://dx.doi.org/10.1016/j.rse.2010.05.003

Guerschman, J.P., Paruelo, J.M., Di Bella, C., Giallorenzi, M.C., Pacin, F. 2003. Land cover classification in the Argentine Pampas using multi-temporal Landsat TM data. *International Journal of Remote Sensing,* 24(17), 3381-3402. http://dx.doi.org/10.1080/0143116021000021288

Hilera González, J.R., Martínez Hernando, V.J. 2000. *Redes neuronales artificiales: fundamentos, modelos y aplicaciones*. Madrid, España: Alfaomega Ra-Ma.

Ikiel C., Ustaoglu, B., Dutucu, A.A., Kilic, D.E. 2013. Remote sensing and GIS-based integrated analysis of land cover change in Duzce plain and its surroundings (north western Turkey). *Environmental monitoring and assessment,* 185(2), 1699-1709. http://dx.doi.org/10.1007/s10661-012-2661-6

Marini, M.F., Vergara, M.F., Krüger, H. 2007. Determinación del uso de la tierra en el partido de Guamini (Argentina) mediante un estudio multitemporal con imagenes Landsat. *Revista de Teledetección,* 27, 80-88. Available at http://www.aet.org.es/revistas/revista27/AET27-08.pdf (accessed December 2015)

Meliadis, I., Miltiadis, M. 2011. Multi-temporal Landsat image classification and change analysis of land cover/use in the Prefecture of Thessaloiniki, Greece. *Proceedings of the International Academy of Ecology and Environmental Sciences,* 1(1), 15-25. Available at http://www.iaees.org/publications/journals/piaees/articles/2011-1(1)/Multi-temporal-landsat-image.pdf (accessed July 2015).

Ministerio de Agricultura, Ganadería y Pesca de la Nación. 2014. Sistema Integrado de Información Agropecuaria. Buenos Aires, Argentina. Available at http://www.siia.gov.ar/_apps/siia/estimaciones/estima2.php (accessed March 2015).

Monserud, R.A., Leemans, R. 1992. Comparing Global Vegetation Maps with the Kappa Statistic. *Ecological modelling,* 62(4), 275-293. http://dx.doi.org/10.1016/0304-3800(92)90003-W

Moreno-Ruiz, J., Arbelo, M., García-Lázaro, J., Riaño-Arribas, D. 2014. Desarrollo de una metodología para la detección de cambios de la cubierta vegetal en series temporales de imágenes de satélite diarias. Aplicación a la detección de áreas quemadas. *Revista de Teledetección,* 42, 11-28. http://dx.doi.org/10.4995/raet.2014.2280

Murthy, C.S., Raju, P.V., Badrinath, K.V.S. 2003. Classification of wheat crop with multi-temporal images: performance of maximum likelihood and artificial neural networks. *International Journal of Remote Sensing,* 24(23), 4871-4890. http://dx.doi.org/10.1080/0143116031000070490

Nolasco, M., Willington, E.A., Bocco, M. 2014. Clasificación del uso de suelo en agricultura a partir de series temporales de imágenes LANDSAT. Proceedings 43JAIIO y VI Congreso Argentino de AgroInformática 1: 64-73. Available at http://43jaiio.sadio.org.ar/proceedings/CAI/6.pdf (accessed July 2015).

Observatorio de Economías Regionales. 2013. La agricultura Argentina en cifras. ACOVI, Mendoza, Argentina. Available at http://www.acovi.com.ar/observatorio/wp-content/uploads/2014/06/la-agricultura-argentina-en-cifras.pdf (accessed July 2015).

Willington, E., Nolasco, M., Bocco, M. 2013. Clasificación supervisada de suelos de uso agrícola en la zona central de Córdoba (Argentina): comparación de distintos algoritmos sobre imágenes Landsat. Proceedings 42JAIIO y V Congreso Argentino de AgroInformática 1:207-216. Available at http://42jaiio.sadio.org.ar/proceedings/simposios/Trabajos/CAI/17.pdf (accessed July 2015).